Research Article

Pharmaceutical BIOPROCESSING

Steady-state biofilm cultivation of *Aspergillus niger* D15 in a ceramic capillary membrane bioreactor

Aim: Bioreactors are an essential component in every biotechnological process. Due to the multitude of different microbial and mammalian organisms used for production of complex products, novel concepts for customized cultivations are necessary. **Results:** A ceramic capillary-based bioreactor enabling a novel approach for steady-state biofilm cultivation is presented. A model for the determination of the efficiency of this system was developed by comparing its productivity to conventional stirred tank reactors using the production of recombinant xylanase by *Aspergillus niger* D15 (*xyn2*) as a model process. **Conclusion:** The presented bioreactor provides an ideal platform for the cultivation of shear-sensitive, filamentous growing microorganisms producing valuable secreted secondary metabolites or recombinant products.

Christian Endres[1,2], Sheena Janet Fraser[2], Wade Edwards[2], Sascha Beutel[1] & Thomas Scheper*[,1]

[1]Institut für Technische Chemie, Leibniz Universität Hannover, Callinstr. 5, 30167 Hannover, Germany

[2]Quorusbiotech (Pty) Ltd, PO Box 13236, Mowbray 7705, Cape Town, Western Cape, South Africa

*Author for correspondence: scheper@iftc.uni-hannover.de

Background

Compared with conventional stirred tank reactors (STRs), an important advantage of membrane-based bioreactors is the provision of an artificial environment for an increased biomass density and enhanced productivity. This artificial environment can further be specified as a platform, which combines biological reactions with membrane separations [1].

Membrane-based bioreactors are generally comprised of independent delivery and removal streams, allowing cell retention and product extraction. Two individual compartments, the extracapillary space (ECS) and intracapillary space (ICS), are separated by the membranes [2,3]. Cells are predominantly grown in the ECS. Additionally, two distinct cycling pathways ensure consistent operation: one is used for medium delivery through or from the ICS and the other is used for inoculation or product removal from the ECS (Figure 1). Major advantages of this configuration are the possibilities of immediate product removal and adjustment of product concentration through variation of the delivery rate. Constant and immediate product removal can additionally be of significant importance when the products are either unstable or lead to product inhibition [4].

First-generation membrane bioreactors relied on diffusion-based mass transfer through the membranes. This operating principle, however, can lead to insufficient aeration, inhomogeneous production and insufficient removal of toxic by-products. To circumvent these problems, second-generation membrane reactors have been developed [5]. These systems are comprised of additional expansion compartments for each supply and removal pathway. However, a disadvantage of such a closed-loop operation is the inability to extract sufficient amounts of biomass to determine growth and viability [5]. These factors can only be assessed indirectly by measuring metabolic activities such as oxygen and glucose consumption. Cell counts can only be performed in end point analysis negating online batch-to-batch comparisons.

Industrial applications for membrane bioreactors have increased significantly over the past two decades and originate from applications such as hemodialysis [6], desalination of seawater or wastewater treatment [7]. Applications for other areas of biotechnology are promising, however, to date only a few examples have been reported [8]. Such biotechnological processes utilize membrane

FUTURE SCIENCE part of fsg

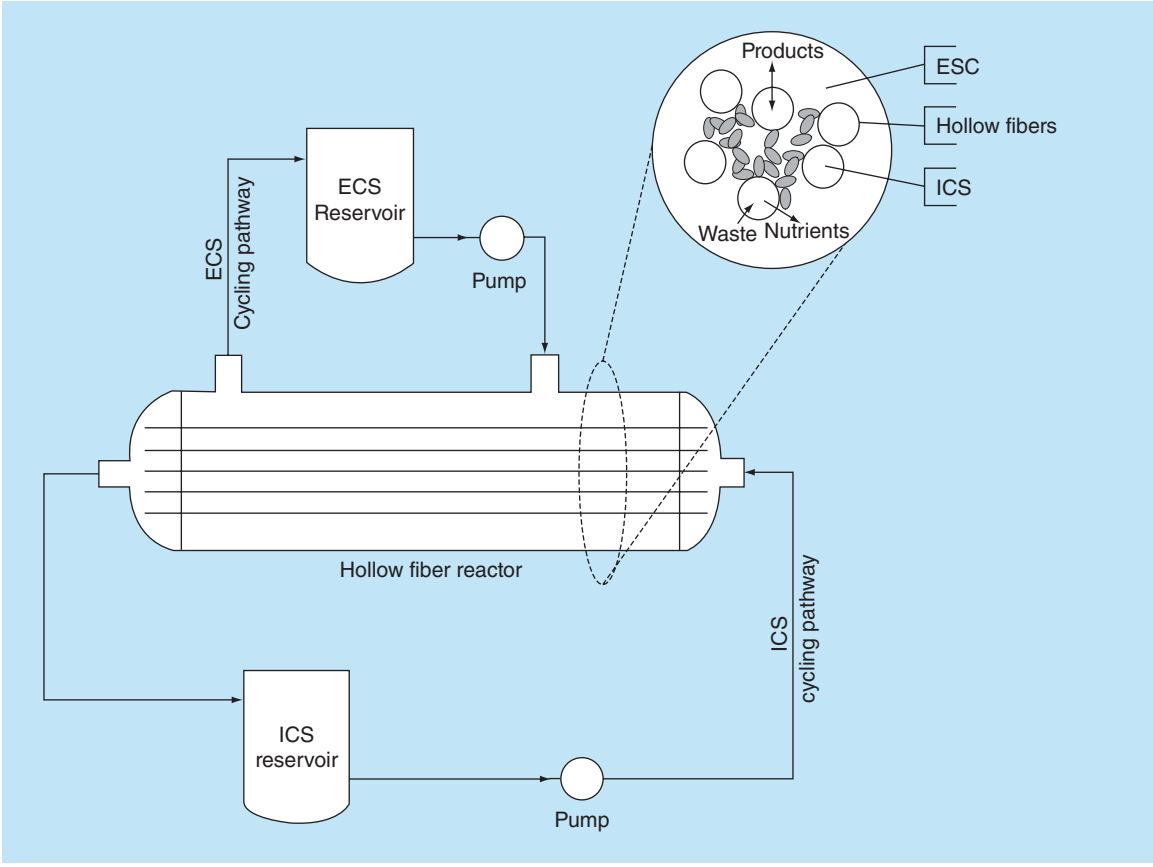

Figure 1. Schematic of a hollow fiber membrane reactor process showing the individual fluid cycles: intracapillary space pathway for medium delivery and extracapillary space pathway for inoculation or product removal.
ECS: Extracapillary space; ICS: Intracapillary space.

reactors, for example, for the production of biosurfactants [9] or the continuous production of (S)-styrene oxide by recombinant *Pseudomonas* sp. [10]. Membrane-based bioreactors are also used in mammalian cell cultivations and in tissue engineering [11,12].

The production of **secondary metabolites** from filamentous microorganisms using membrane-based bioreactors has been described by various groups [13–15]. Here, shear stress-sensitive microorganisms are immobilized onto the outer surface of capillary membranes acting as a support matrix [16] and are grown in a fully aerated environment while constantly supplied substrates enable a continuous production of valuable secondary metabolites [17] or recombinant products [18,19]. Such processes follow the gradostat concept, which describes the formation of nutrient and oxygen gradients across the biofilm to facilitate steady-state cultivations [20]. Such processes are typically performed in a **membrane gradostat reactor**. For example, Govender *et al.* [21] used *Phanerochaete chrysosporium* ME446 immobilized onto vertically orientated capillary polysulfone membranes for the production of manganese peroxidase. De Jager *et al.* modeled the biphasic growth of actinorhodin producing *Streptomyces coelicolor* A3(2) immobilized onto ceramic membranes [22].

Filamentous fungi have well-developed biosynthetic pathways for the high-level secretion of a large variety of proteins and are increasingly being exploited as expression systems for the production of complex heterologous proteins [29]. Especially the well-studied *Aspergillus niger* is commonly used for the expression of industrial proteins and antibody fragments [30]. In this study, the production of recombinant xylanase by *A. niger* D15 (*xyn2*) is used as a model process to evaluate the efficiency of

Key term

Membrane bioreactor: A bioreactor system in which a microorganism is grown on the outer surface of a membrane which retains the cells but enables the permeation of nutrients.

Secondary metabolite: Compounds produced by microorganisms in response to nutrient limitations. Such compounds are mostly secreted and are unessential for cell growth and cell reproduction.

Membrane gradostat reactor: A modification of a membrane bioreactor in which a biofilm is immobilized and grown on the outer surface of a capillary membrane. Gas and liquid flow are bidirectional, formed gradients within the biofilm are oppositely directed (outside-in and inside-out). Within the biofilm, the different cell growth phases are spatiotemporally separated.

the presented capillary ceramic membrane reactor, while reactors commonly used in first stage bioprocess development have been used for benchmarking.

Materials & methods

Microorganism & media

The secretion of recombinant xylanase by *A. niger* D15 (*xyn2*) was achieved by overexpression of the *Trichoderma reesei* xylanase II gene (*xyn2*) in the fungal genome of *A. niger* D15 [23]. This modified strain was provided by Synexa Life Sciences (Pty) Ltd (Cape Town, South Africa), to whom it was given by Willem van Zyl *et al.* (Stellenbosch University, South Africa) for demonstration purposes only.

Spore suspensions of *A. niger* D15 (*xyn2*) were prepared from malt extract agar dishes (in g/l): malt extract 20, bacterial peptone 1, glucose 20 and agar 150. The agar dishes were inoculated with spores from stock cultures and incubated at 30°C for 7 days. Formed spores were suspended in d-H_2O (Arium, Sartorius Stedim Biotech GmbH, Goettingen, Germany), centrifuged, concentrated and finally stored in 20% glycerol at -20°C.

2× Minimal medium was used as cultivation medium in all processes and consisted of (in g/l): yeast extract 10, glucose 20, sodium nitrate 6, bacterial peptone 1 and trace elements solution 1 ml/l. The trace elements solution consisted of (in g/l): $ZnSO_4 \cdot 2H_2O$ 20.13, $MnCl_2 \cdot 2H_2O$ 4.95, $FeSO_4 \cdot 7H_2O$ 5.04, $CoCl_2 \cdot 6H_2O$ 1.69, $CuSO_4 \cdot 5H_2O$ 1.6, $NaMoO_4 \cdot 2H_2O$ 1.5, Na-EDTA 129.54. Unless stated otherwise, all chemicals were obtained from Sigma-Aldrich Chemie Gmbh (Munich, Germany).

Xylanase activity assay

endo-1,4-β-D-xylanase activity in the fermentation broth and permeate was determined photometrically using the Azo-Xylan (Birchwood) assay (Megazyme International Ireland Ltd, Bray, Ireland). Briefly, after

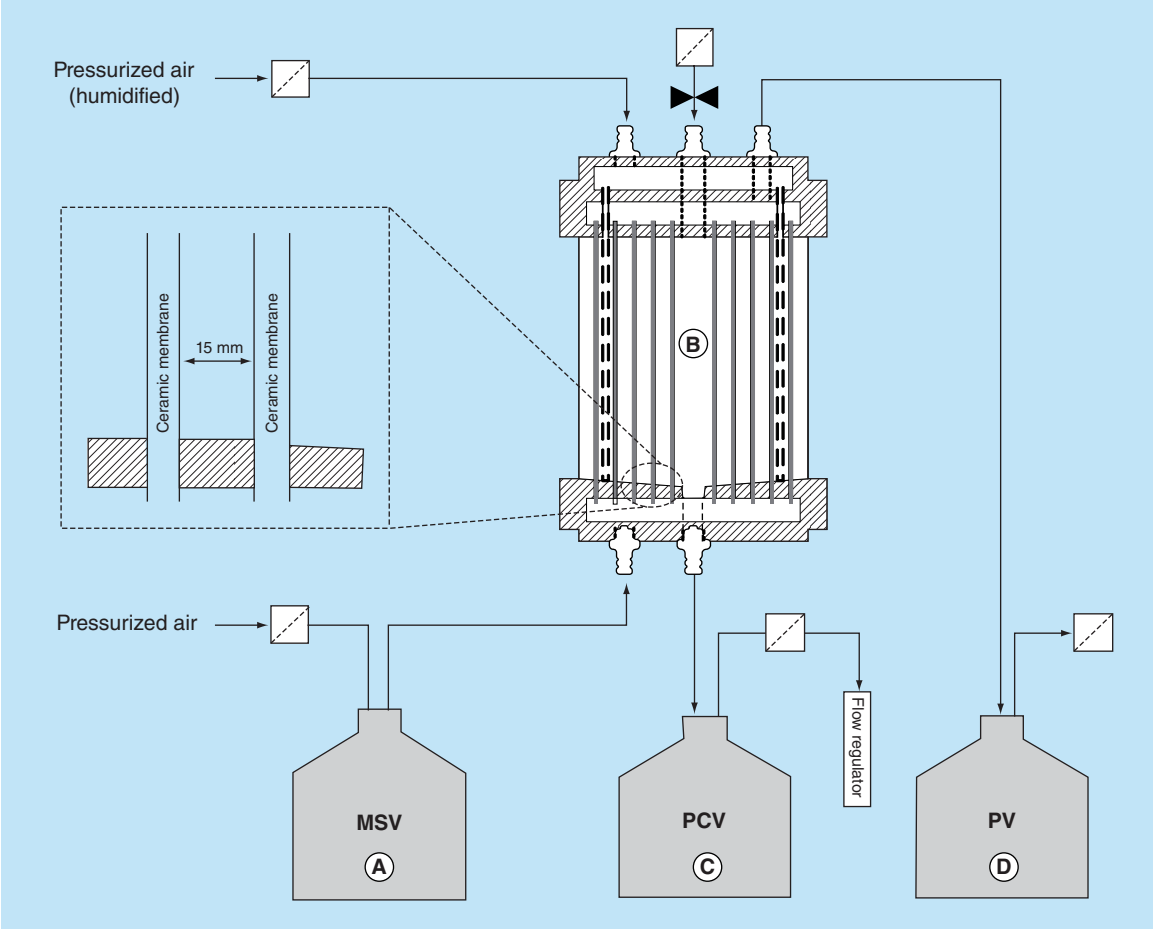

Figure 2. Quorus gas–liquid–solid bioprocess. By applying pressure onto the medium supply vessel **(A)**, medium flows unidirectionally into the intracapillary space of the reactor **(B)**, through the membranes and subsequently perfuses the biofilm. It exits the reactor as spent medium, enriched with secreted products into the product collection vessel **(C)**. Inoculation is accomplished by transferring the inoculum into the extracapillary space with subsequent priming into the intracapillary space.
MSV: Medium supply vessel; PCV: Product collection vessel; PV: .

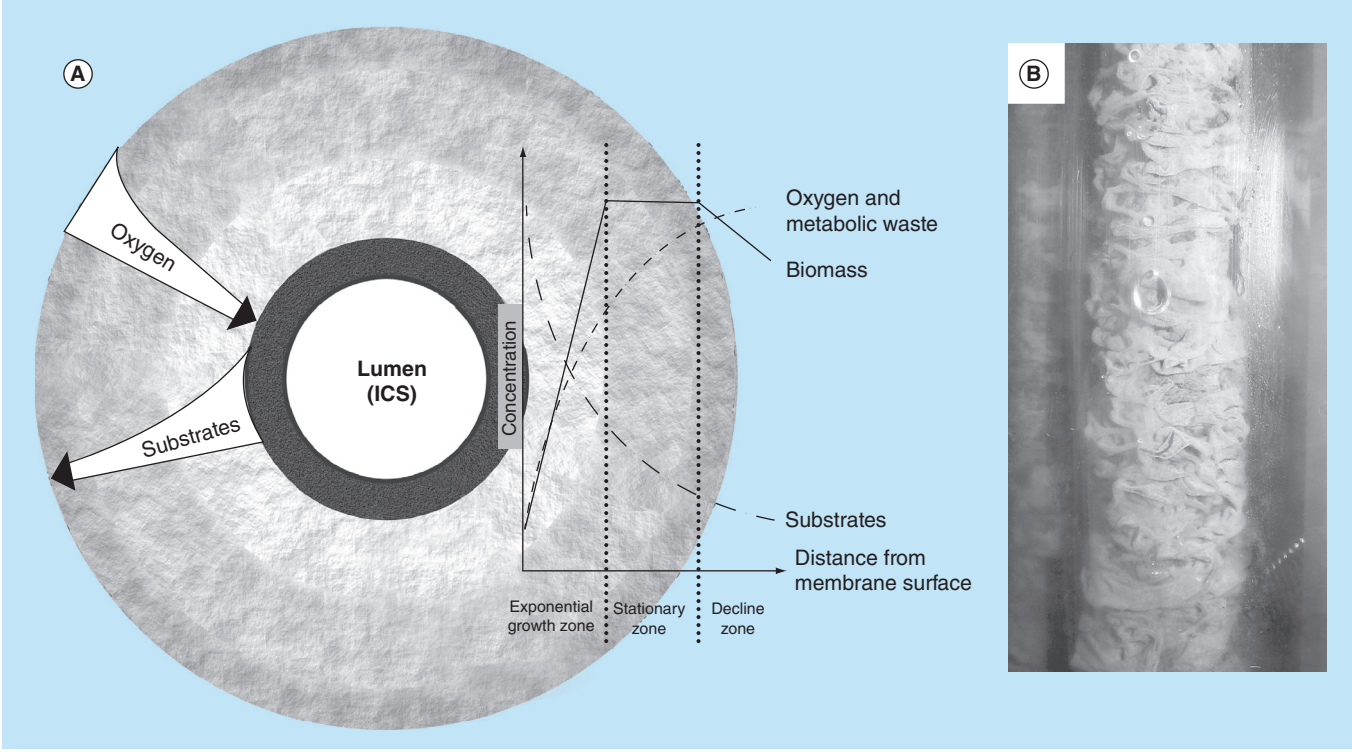

Figure 3. Gas–liquid–solid biofilm growth. **(A)** Cross section of biofilm surrounding the ceramic membrane. Oxygen and nutrient gradients formed during biofilm formation around the ceramic membranes in the aerobic Quorus gas–liquid–solid bioprocess. Spatiotemporally distributed growth zones are observed: exponential growth zone, stationary zone and decline zone. **(B)** *Aspergillus niger* D15 (*xyn2*) biofilm after 12 days of cultivation in a Quorus gas–liquid–solid system with an average thickness of 0.4 ± 0.1 cm from the membrane surface.
ICS: Intracapillary space.

incubation of Azo-Xylan with *endo*-xylanase, the substrate is depolymerized. Upon addition of ethanol, low-molecular weight dyed fragments remain in solution while high-molecular weight fragments precipitate and are removed by centrifugation. By measuring the absorbance of the supernatant at 590 nm the endo-xylanase activity can be determined by referencing the results to the *Trichoderma longibrachiatum* xylanase standard curve using Equation 1 (for 0.5 ml assays):

$$\frac{\text{Units}}{\text{ml}} = \left(97.7 \cdot \text{Abs}^2 + 178 \cdot \text{Abs} + 3.1\right) \cdot \frac{\text{dilution}}{10}$$

Batch cultivation parameters

Batch cultivations for benchmarking purposes were performed in 300 ml nonbaffled shaking flasks, a 3 l total capacity Biostat A plus (Sartorius Stedim Biotech GmbH, Goettingen, Germany) STR with a 1.8 l working volume and a 15 l total capacity Biostat C (B. Braun Biotech GmbH, Melsungen, Germany) STR with a 10 l working volume. Batch processes in different scales have been chosen for benchmarking purposes and to represent standard configurations used in bioprocess development. Nutrient conditions were identical by using freshly prepared and sterile filtered 2× minimal medium medium. All batches were inoculated with identical spore preparations of *A. niger* D15 to a final concentration of 1×10^5 spores per ml working volume. All cultivations were carried out at 30°C. Agitation in the Biostat reactors was provided by two (Biostat A plus) and three (Biostat C) Rushton impellers operated at 400 rpm. Aeration was maintained at 1 vvm. Flask cultures were agitated using an orbital shaker at 200 rpm. Initial pH in all cases was 6.5 and remained during cultivation within the range of pH 5.0–6.0 as optimal for maximum xylanase activity [23] without the necessity for pH control. Biostat cultivations were treated with 0.2 ml/l antifoam (Tego KS911, Goldschmidt, Essen, Germany) to limit culture fluid overflow.

Ceramic membrane reactor operation parameters

The single-use ceramic membrane reactor prototype Quorus gas–liquid–solid (GLS) used in this study was kindly provided by Synexa Life Sciences (Pty) Ltd and consisted of 50 vertically aligned ceramic membranes housed within a cylindrical manifold with a total capacity of 2.05 l. The ceramic membranes (OD = 4.0 mm, ID = 3.8 mm, mean pore size of inner coating: 40 nm) with an accessible length of 19.5 cm are dis-

tributed evenly in a hexagonal arrangement with an intermembrane spacing of 15 mm.

The Quorus GLS bioreactor was inoculated with a spore preparation of *A. niger* D15 to a final concentration of 1 × 10^5 spores per ml reactor capacity. Sterile filtrated 2× MM medium was used for nutrient delivery. The reactor was incubated at 30°C, airflow was set to 2 l/min, the base operating pressure was adjusted to 0.3 bar and the medium supply rate was automatically controlled at 50 ml/h.

Aerobic process for steady-state biofilm cultivation & recovery of secreted products

The disposable Quorus GLS bioreactor is designed for the cultivation of aerobic and filamentous growing organisms. Within these bioreactors, biomass is immobilized and cultured as a biofilm on the outer surface of vertically orientated ceramic capillary membranes. Biofilm growth occurs at the GLS interface – within the ECS – and is supported by a constant supply of growth medium via the ICS and a constant aeration across the outer biofilm surface.

The bioprocess utilizes pneumatic pressure for medium delivery, aeration and product removal. By applying pressure onto a medium supply vessel (Figure 2A), medium flows unidirectionally into the ICS of the reactor chamber (Figure 2B). With the ICS being operated dead-end, medium is transported convectively through the capillary walls, perfuses the immobilized microorganism and emerges as spent and product enriched permeate the reactor through the ECS and is collected in the product collection vessel (Figure 2C). Aeration of the ECS is accomplished by pressurized and humidified air flowing through the ECS at a constant volumetric rate and backpressure, exiting the reactor at the same outlet as the permeate. Homogeneous ECS aeration is aided by distinct distribution manifolds evenly positioned within the hexagonal alignment of the capillaries.

The permeation rate of medium from the ICS into the ECS is proportional to the transmembrane pressure (TMP) – the pressure differential between the ICS and ECS compartments. However, biofilm density and thickness around the capillaries directly affect overall nutrient delivery rates. With increasing biofilm density and thickness, resistance to flow is increased and therefore ICS pressure is automatically adjusted to facilitate constant nutrient delivery rates to maintain steady-state biofilm growth.

For inoculation the system is operated inversely. The ECS is aseptically filled with the inoculum, preferably a spore suspension, followed by application of pressurized air to drive the suspension medium into the ICS and subsequently into the prime vessel (Figure 2D),

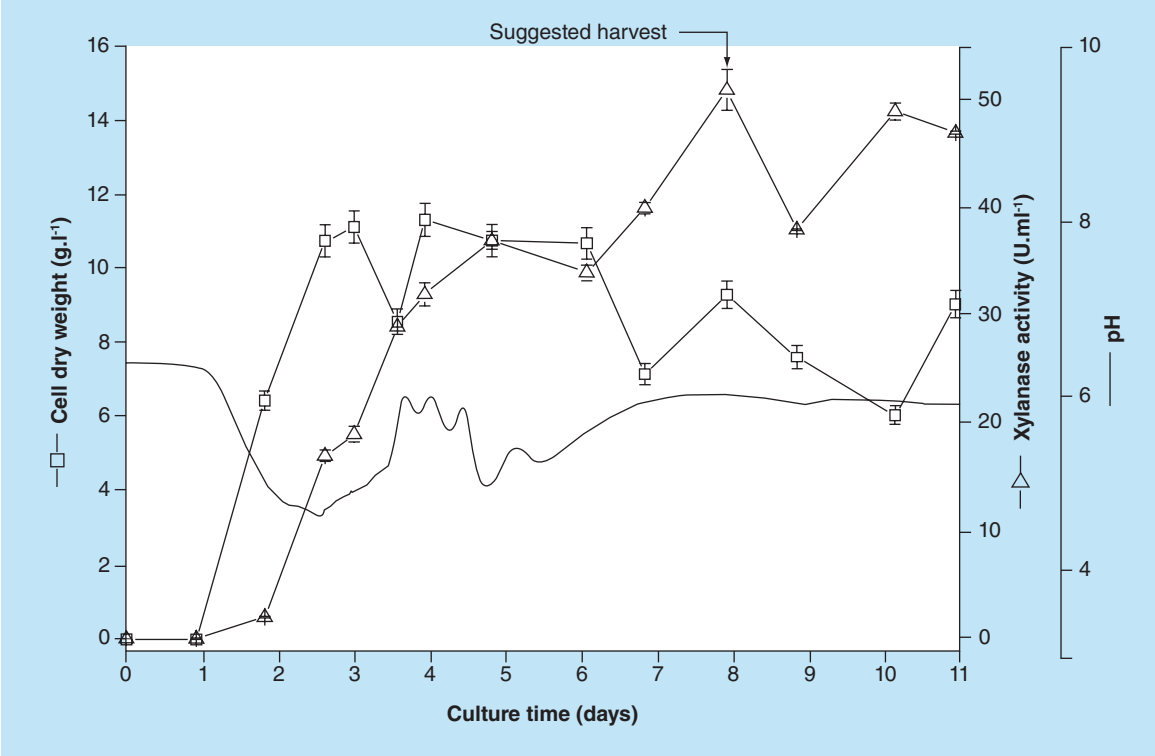

Figure 4. Results of a 1.8-l Biostat A plus cultivation (30°C, 400 rpm, 1 vvm) of *Aspergillus niger* D15 (*xyn2*) to produce xylanase and time course of cell dry weight (open rectangles) and pH (black line). After 7.9 days the highest xylanase activity (51 ± 1.9 U/ml; open triangles) is reached.

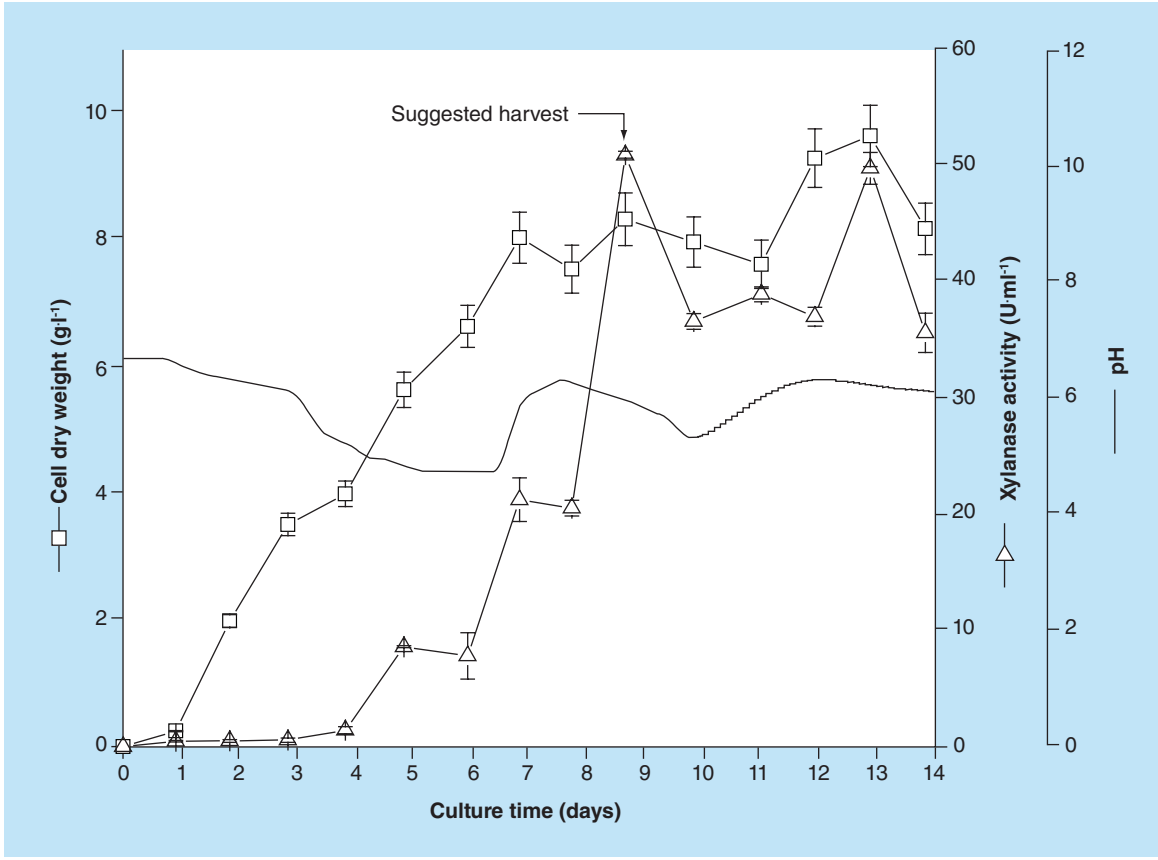

Figure 5. Ten-liter Biostat C cultivation (30°C, 400 rpm, 1 vvm) of *Aspergillus niger* D15 (*xyn2*) to produce xylanase and time curse of cell dry weight (open rectangles) and pH (black line). After 8.7 days the highest xylanase activity (51 ± 0.4 U/ml; open triangles) is reached.

thus immobilizing the microorganism onto the membranes. Sporulation and subsequent biofilm formation is then induced by reverting back to regular operation. Here, nutrient medium flows unidirectionally from the ICS through the porous walls of the membranes and perfuses the biofilm, while the biofilm is aerated by humidified air flowing across its surface.

Initial biofilm growth kinetics are comparable to the patterns described for batch cultivations [22]. With increasing biofilm thickness and under a given substrate feed rate the biofilm will enter steady state [24]. During this process radial nutrient and dissolved oxygen gradients are established across the biofilm (Figure 3). Such steady-state biofilms are showing a spatiotemporal distribution of the different cell growth phases in a complex 3D structure. First, a thin zone of cells close to the membrane surface is maintained in exponential growth by a replenishing supply of nutrients. Here, a network of hyphae differentiated for penetrative growth and adapted for the utilization of easily accessible nutrients, thus providing a continuous supply of precursors for secondary metabolite formation [25]. With decreasing nutrient concentration cells will enter into and are maintained in stationary growth, while nutrient limited conditions induce secondary metabolite production. The slope of the nutrient gradient is generally limited by the highly complex three-dimensional biofilm structure and its ability to translocate nutrients through the filamentous hyphal structure [26]. Nutrient concentration may be depleted in a thin zone on the exterior of the biofilm, resulting in sporulation, cell death and lysis (decline zone).

Dissolved oxygen transport to the cells occurs at the outer boundary layer of the biofilm with humidified air flowing across its surface. The rate of oxygen transport into the biofilm can be determined by linking the convective and diffusive mass transport rates [27]. Oxygen consumption within the biofilm will increase with biofilm thickness, leading to an oxygen gradient from the exterior of the biofilm toward the membranes lumen [27]. Both gradients will influence the maximum biofilm diameter. Metabolic waste and secreted products are removed from the biofilm along with the spent medium, thus limiting the degeneration or conversion of the target product, by flowing down on the exterior biofilm surface, to finally emerge from the reactor's ECS along with the airstream.

Through a controlled supply of nutrients the biofilm will be maintained at a constant thickness and active biomass as well as product formation is retained in steady state. Overall process kinetics [22] and biofilm thickness are furthermore dependent on the operating conditions and the specific microorganism. While the impact of nutrient gradients on the biofilm physiology and process kinetics has been studied for the production of manganese peroxidase from *P. chrysosporium* [15,21], its influence on *A. niger* remains subject to further research.

Process scalability

Initial development for the Quorus GLS processes is performed using single-fiber reactor modules. The overall process setup for single-fiber reactors is virtually identical to that shown in Figure 2. Single-fiber reactors consist of a single capillary membrane encased within a cylindrical reactor module with a total volume of 20 ml [22]. Dimensions and characteristics of capillary membranes used in single-fiber reactors are identical to those integrated into Quorus GLS multifiber reactors. Parallel operation of single-fiber reactors as well as experimental design techniques are used to determine key process parameters affecting biofilm formation and process productivity, including: incubation temperature, medium composition and operating pressures. Process conditions developed for single-fiber reactors can be scaled directly to multifiber processes.

Govender *et al.* [28] report a sevenfold increase in manganese peroxidase production from *P. chrysosporium* ME446 with a tenfold increase in bioreactor size.

Linear scale-up of reactor process parameters is determined by the number of capillary membranes housed within the reactor chamber. Quorus module design ensures uniform fluid distribution within membrane ICS and homogeneous aeration of the ECS. Computational fluid dynamics of reactor designs are currently being used to develop larger scale reactor modules.

Results

Bioreactor cultivation of *Aspergillus niger* D15 (*xyn2*)

Cultivations of *A. niger* D15 (*xyn2*) in shaking flasks were carried out for 8.9 days and reached a maximum xylanase activity of 41 ± 2 U/ml. Comparative experiments in the Biostat A plus and Biostat C STRs were carried out for a period of 11 days and 14 days, respectively. Maximum xylanase activities of 51 ± 1.4 U/ml were reached within the stationary growth phase after

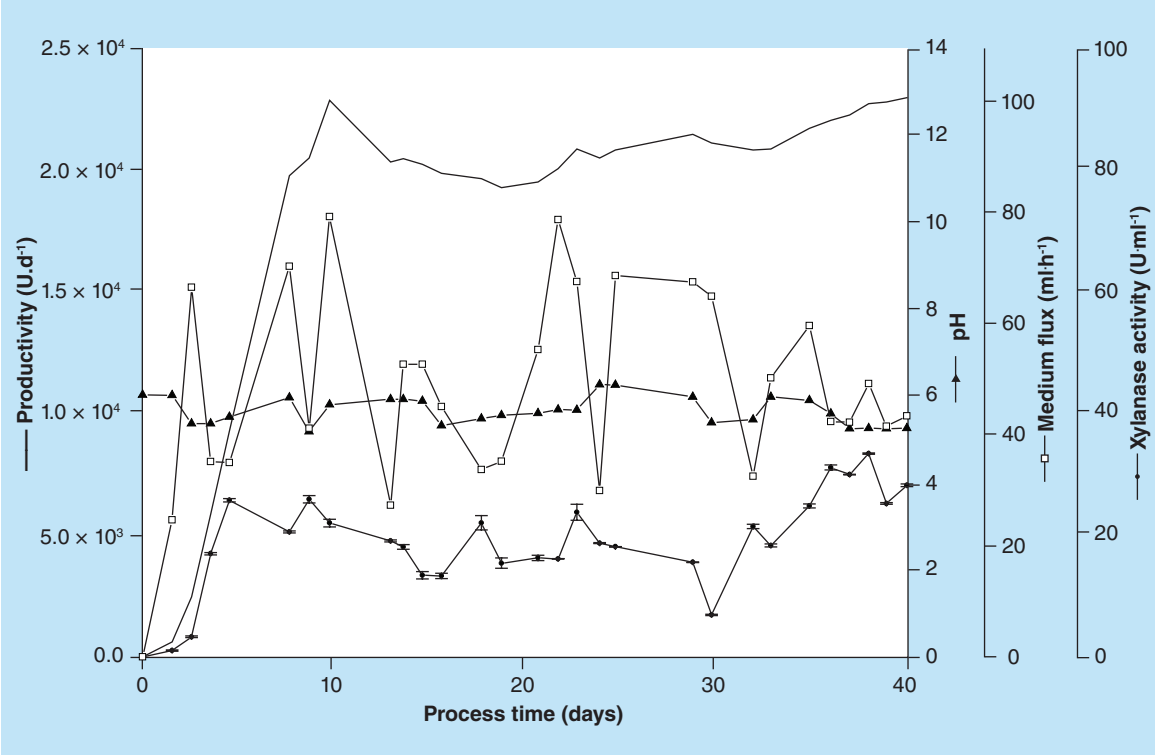

Figure 6. Continuous production of xylanase by *Aspergillus niger* D15 (*xyn2*) using a Quorus gas–liquid–solid 2-l – 50-membrane bioreactor. Displayed are xylanase activity (black dots), pH (black triangles), average medium flux (open rectangles) and Quorus gas–liquid–solid productivity (black line). The productivity stabilized after approximately 10 days with a constant production of about 2.1 ± 0.1 × 10^4 $U_{xylanase}$/day.

Table 1. Results from *Aspergillus niger D15* (*xyn2*) cultivations to produce xylanase in various reactor systems.

Reactor system	Culture time (days)	Total yield (U)	Averaged activity (U/l_{Medium})
Shaking flasks	8.9	$2.4 \pm 0.1 \times 10^3$	$4.0 \pm 0.3 \times 10^4$
Biostat A plus	7.9	$9.2 \pm 0.3 \times 10^4$	$5.1 \pm 0.2 \times 10^4$
Biostat C	8.7	$5.1 \pm 0.1 \times 10^5$	$5.1 \pm 0.3 \times 10^4$
Quorus GLS 2 l (50 membranes)	40	$9.2 \pm 0.3 \times 10^5$	$1.9 \pm 0.4 \times 10^4$

GLS: Gas–liquid–solid.

7.9 days in the Biostat A plus (Figure 4) and 8.7 days in the Biostat C (Figure 5). The difference in peak production times resulted from an oxygen limitation in the Biostat C after 2.5 days leading to a reduced growth rate when compared with the Biostat A plus (data not shown). The timestamps of xylanase peak activities are considered to be the optimal harvesting times and are used for all subsequent calculations.

The continuous cultivation of *A. niger* D15 using the Quorus GLS bioreactor was carried out over a period of 40 days and a total of 48.2 l medium was used. After approximately 10 days, the cultivation in the GLS reactor reached steady state, where productivity stabilized at approximately $2.1 \times 10^4 \pm 0.1$ U/day (Figure 6). After entering this stable production phase the biofilm showed a deep brownish pigmentation with negligible sporulation, which intensified after 25 days of operation. Biofilm thickness stabilized after 15 days and showed a conical tapering in diameter from top (1.2 cm) to bottom (1.8 cm) of the vertically orientated membranes.

Within the first 24 h after inoculation, medium flux was limited to 25 ml/h (0.5 ml/h per membrane) to prevent spores and loosely adhered mycelia being washed off the membranes. From day 2 till the end of the cultivation, medium delivery was automatically controlled at a rate of 50 ml/h: transmembrane pressure was adjusted automatically and varied between 0.02 and 0.1 bar. Over and under shooting (Figure 6) resulted from an intentionally set slower PID controller responses of the medium pressure inlet valve.

Bioprocess efficiency

During conventional batch fermentation, biomass is concentrated toward a maximum cell titer resulting from the amount of nutrients supplied. Additionally, product formation will increase during the process until a maximum product concentration or working volume-dependent product output is reached. This is illustrated by the similar maximum xylanase activities obtained for the Biostat A plus and Biostat C bioprocesses (Table 1).

Biofilm growth in the Quorus GLS bioreactor is self-regulated: it is maintained by the amount of nutrients supplied to the biomass through nutrient flux [16]. As oxygen supply and nutrient delivery rates can be adjusted to fit process requirements, the biofilm thickness is limited by the organism itself and by the extent of available space around the membranes. It reaches a process-dependent thickness, in case of *A. niger* as presented in this study a diameter of 1.2–1.8 cm. The optimal biofilm thickness and the optimal membrane spatial alignment, as well as set nutrient supply rate to sustain a biofilm of such thickness is process dependent and can generally be adjusted to match process specifications. In contrast to STRs, product is not concentrated, but rather continuously removed from the biomass thereby sustaining maximum productivity of the biofilm. This results in a lower volumetric productivity when compared with a STR.

A valid parameter for the comparison of bioprocesses is volumetric productivity. While in batch fermentation the volume of the growth medium is fixed by the STR's working volume, media volumes in Quorus operation will increase over time while the product concentration

Table 2. Results from *Aspergillus niger* D15 (*xyn2*) cultivations to produce xylanase in various cultivation vessels.

	Culture time (days)	Overall productivity (U /day)	Volumetric production rate (U/l_{Medium}/day)	Production rate per reactor capacity ($U/l_{Reactor}$/day)
Shaking flasks	8.9	$2.0 \pm 0.1 \times 10^2$	$4.5 \pm 0.1 \times 10^3$	$5.1 \pm 0.2 \times 10^2$
Biostat A plus	7.9	$1.2 \pm 0.1 \times 10^4$	$6.4 \pm 0.1 \times 10^3$	$3.9 \pm 0.2 \times 10^3$
Biostat C	8.7	$5.9 \pm 0.1 \times 10^4$	$5.1 \pm 0.1 \times 10^3$	$3.9 \pm 0.1 \times 10^3$
Quorus GLS 2 l (50 membranes)	40	$2.3 \pm 0.1 \times 10^4$	$2.5 \pm 0.1 \times 10^{3,\dagger}$	$1.1 \pm 0.1 \times 10^4$

All values are averaged to the whole process time. Given values represent mean values and standard deviations.
†Based on the use of 10-l medium within a stable production phase to compare to STR batches.
GLS: Gas–liquid–solid; STR: Stirred tank reactor.

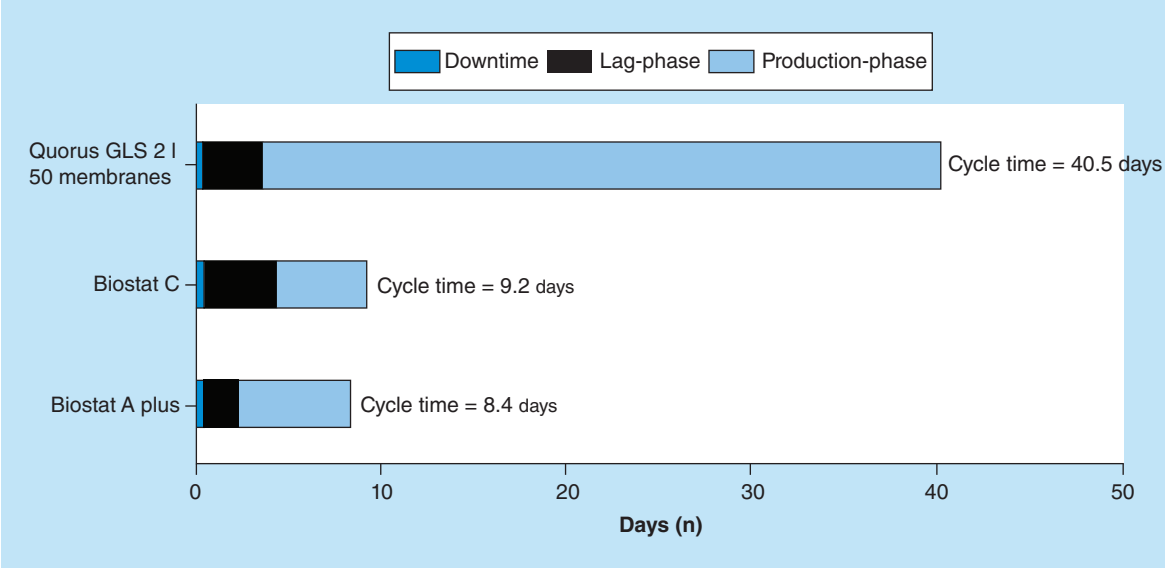

Figure 7. Total cycle time of the reactor-specific production cycles for the compared bioreactors. Each production cycle is composed of downtime, lag phase and production phase.

in the product stream remains constant. For a suitable comparison the volumetric production rate for the Quorus system was instead calculated using a defined volume of medium: as the Biostat C working volume was 10 l, the volumetric productivity of the Quorus GLS was calculated over a period of time within the stable production phase, where 10 l of medium were used. As it can already be anticipated from its lower product titer (Table 1), the average volumetric production rate of $2.4 \times 10^3 \pm 0.1$ U/l_{Medium}/day of the Quorus GLS is comparably lower than in the benchmark systems (Table 2).

The performance of a reactor system can alternatively be described by referencing its productivity to the total reactor volume. In this study it has been normalized to 1 l of reactor capacity. Even though overall productivity and volumetric productivity of the Quorus GLS were comparably lower than in the larger Biostat C, the efficiency of the biofilm cultivation can be shown by its high productivity per reactor capacity (Table 2). However, increasing the working volume of the STRs Biostat A plus and C will result in a higher productivity per reactor capacity, but at the cost of reducing crucial headspace.

Long-term process performance

To evaluate the process performance of the Quorus GLS in long-term operation and reference it to the benchmark processes, a productivity model has been developed considering an overall process time frame of 180 days.

In this analysis, initial xylanase production in the Quorus GLS was terminated after 40 days (Figure 6), which included a 37.4 days uninterrupted production phase. While product removal in the Quorus GLS can be accomplished continuously within this production phase, harvesting in the STR's Biostat A plus and C can only be performed once and therefore defines the end of their production cycle. For further estimation, a process- and reactor-dependent cycle time describing the complete duration of a single process run is defined. Each production cycle consists of a standardized 12 h downtime for process and reactor setup, a reactor-specific nonproductive lag-phase and a reactor-specific production phase (Figure 7). Within one Quorus GLS production cycle (40.5 days) a total of 4.4 (Biostat C) and 4.8 (Biostat A plus) production cycles can be completed.

Performing all processes with their respective cycle times in the considered time frame of 180 days sequentially would result in a linear scaling or accumulation of their individual productivities (Tables 1 & 2).

However, while total production time in the STRs is fixed by an optimal harvest point, the termination of the Quorus GLS production phase is variable. Such a variation will impact on the total quantity of production cycles that can be undertaken within the estimated period of t = 180 days. The overall productivity of the Quorus system within this time frame will be affected accordingly. In Figure 8A, the Quorus product output was normalized against the total amount of xylanase produced in a Biostat C (stated as productivity ratio R_i), so that the productivity of the Quorus GLS system can be modeled and referenced to the STRs (Equation 2). This was achieved by calculating the product output of the Quorus system, when the duration of the Quorus production phase is increased from

$$t_i^{production} = 0..t(d): \qquad R_i = \frac{P_{exp} \cdot t^{production} \cdot cyc_i}{P_{STR} \cdot t_{exp} \cdot cyc_{STR}}$$

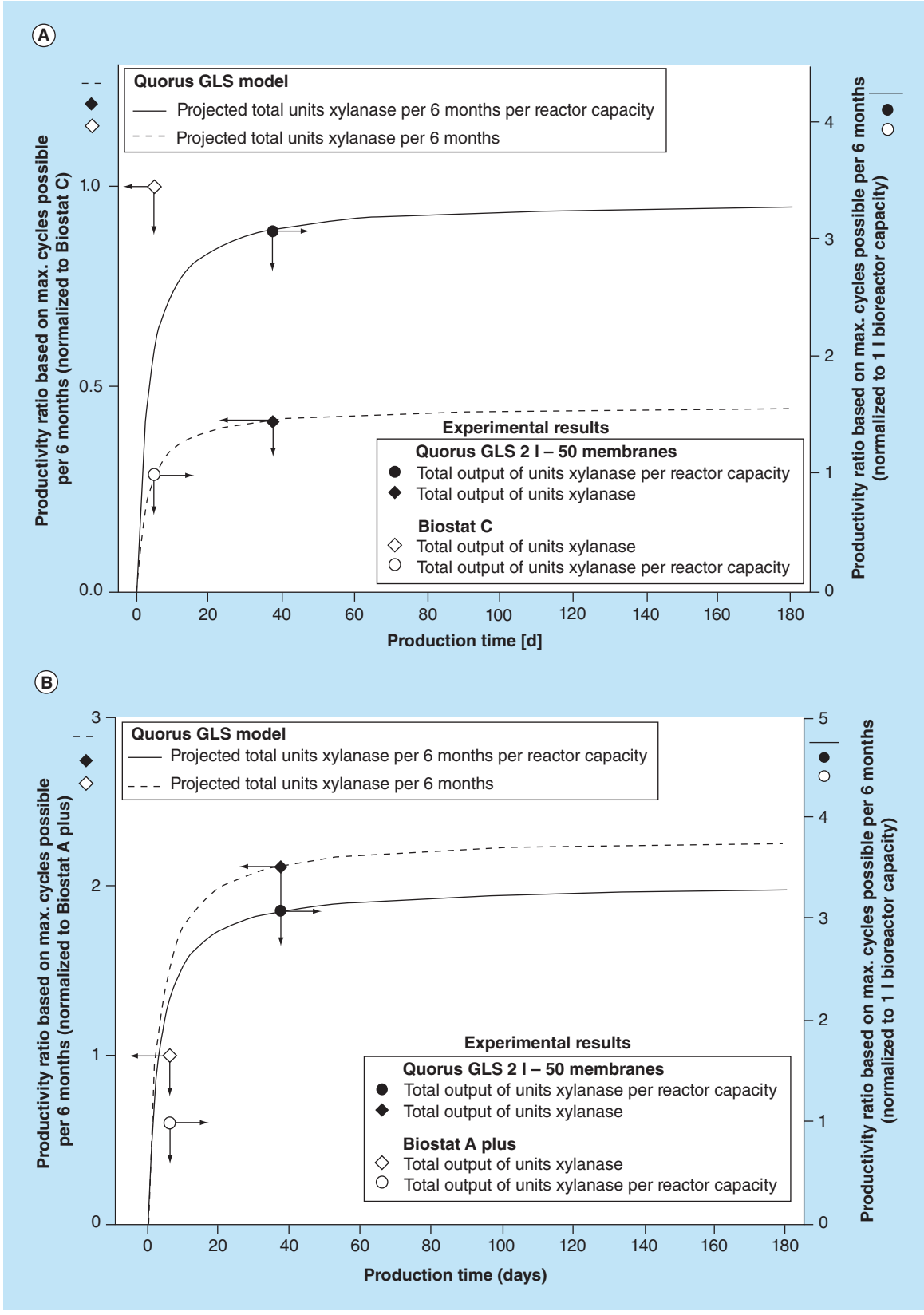
A
Quorus GLS model
Projected total units xylanase per 6 months per reactor capacity
Projected total units xylanase per 6 months
Experimental results
Quorus GLS 2 l – 50 membranes
Total output of units xylanase per reactor capacity
Total output of units xylanase
Biostat C
Total output of units xylanase
Total output of units xylanase per reactor capacity
Productivity ratio based on max. cycles possible per 6 months (normalized to Biostat C)
Productivity ratio based on max. cycles possible per 6 months (normalized to 1 l bioreactor capacity)
Production time [d]
B
Quorus GLS model
Projected total units xylanase per 6 months per reactor capacity
Projected total units xylanase per 6 months
Experimental results
Quorus GLS 2 l – 50 membranes
Total output of units xylanase per reactor capacity
Total output of units xylanase
Biostat A plus
Total output of units xylanase
Total output of units xylanase per reactor capacity
Productivity ratio based on max. cycles possible per 6 months (normalized to Biostat A plus)
Productivity ratio based on max. cycles possible per 6 months (normalized to 1 l bioreactor capacity)
Production time (days)

Figure 8. Modeling of a Quorus gas–liquid–solid cultivation of *Aspergillus niger* D15 (*xyn2*) to produce xylanase (see facing page). Impact of extending Quorus GLS production phase up to 180 days onto the total product output (dashed lines) and space-time yield (black lines) of the Quorus process. These data are superimposed on the actual Quorus GLS and Biostat C **(A)** as well as Biostat A plus **(B)** results: total output of xylanase of the Biostat STRs (open diamonds) and Quorus GLS (black diamonds) as well as the total output of xylanase per liter reactor capacity of the Biostat STRs (open circle) and Quorus GLS (black circle). All values are normalized to the accumulative output of the maximum number of Biostat C and A plus batches over 180 days.
GLS: Gas–liquid–solid; STR: Stirred tank reactor.

where t_{exp} is the duration of the experimental Quorus GLS production phase (days), P_{exp} is the productivity of the experimental Quorus process (U/day), cyc_i is the number of possible Quorus cycles in *t*, P_{STR} is the productivity of the STR batch (U/day) and cyc_{STR} is the amount of possible STR cycles in t.

Figure 8A indicates a dual comparison normalized to the Biostat C: the total product output ratio of xylanase (dashed line) and the productivity ratio based on reactor capacity (black line). The final product output (black diamond) and space-time yield (black circle) of the experimental Quorus GLS process (~41 day cycle time) and Biostat C (~10 day cycle time) (open diamond and open circle) over a 180-day period are marked. Because the Biostat C cycle time is fixed, its productivity remains constant and is used as a baseline Quorus GLS referencing. From the model data superimposed in Figure 8A, it is clear that with shorter Quorus production phases the impact of additional downtime and lag-phase at the start-up of each cycle is apparent. With longer production phases fewer cycles need to be performed and the impact of downtime and lag-phase on productivity is less significant. In this case the product output and productivity per reactor capacity approach a maximum as the production phase extends beyond 60 days, while total product output of the 2 l Quorus GLS will reach not more than 44% of a Biostat C. Quorus GLS productivity per reactor capacity breaks even after a production time frame of 2 days.

Based on above assumptions, Figure 8B shows the impact on total product output and productivity of the Quorus GLS process when varying its production phase and referencing it to the results obtained for the Biostat A plus.

Here, the product output (dashed line) and space-time yield (black line) approach a maximum as the Quorus GLS production phase is extended beyond 80 days. The total product output of the 2 l Quorus GLS breaks even with the Biostat A plus (open diamond) after production times of about 3 days. With production phases longer than 80 days the total xylanase output of the Quorus GLS would be approximately 2.3-times higher than sequentially performed Biostat A plus processes. Productivity per reactor capacity breaks even after a production phases of 2 days and surpasses the Biostat A plus with production phases longer than 21 days.

Conclusion & future perspective

The Quorus GLS reactor system is suited for the continuous cultivation of aerobic and filamentous growing organisms. In contrast to batch-operated STRs, productive biomass is not concentrated toward a nutrient-dependent maximum, but instead immobilized and then grown as a self-regulating biofilm using ceramic capillaries as the immobilization matrix. The GLS process operates according to the gradostat principle, relying on the formation of opposed nutrient and oxygen gradients over the cross section of a biofilm. Products secreted by cultured microorganisms are continuously removed along with the spent medium. The production of xylanase by *A. niger* D15 (*xyn2*) has been used as a model process to describe and determine the Quorus GLS bioprocess performance. Conventional batch processes have been utilized for benchmarking. Product titers in the Quorus GLS cultivations were generally lower than in the benchmark cultivations, but stabilized once the biofilm entered steady state.

While the cycle times for batch-operated reactor systems are determined by culture-specific harvesting times, cycle times in the Quorus GLS can be varied by changing the duration of its production phase with significantly influencing Quorus GLS productivity. By plotting such data as a time course study, break-even points between the individual processes were estimated and stable Quorus GLS production phases, where the expansion of production time will have no increasing effect on process performance were assessed.

It can be reasoned that further optimization of the process parameters for biofilm cultivation of *A. niger* D15 (*xyn2*) would result in increased product titers process productivity. Integration of downstreaming steps into the continuous permeate stream of the Quorus GLS process, for example, separation of sloughed of biomass [17] or trapping of volatile components, would significantly increase the process' economic efficiency.

The continuing effort to explain factors influencing protein expression in foreign hosts and the ongoing drug discovery using microbial natural products as the source of new leads, the commercial potential of unconventional cell types and expression systems is set to increase. Cells not suited to conventional process technologies, however, will lead to expensive process developments and often low product titers – marking such bioprocesses as economically unviable. Bioreactors

offering innovative designs to replicate a more natural growth environment for unconventional cell types, will provide a more efficient platform to derive valuable products from such cells. Knowledge of mass transfer within the biofilms is crucial to understand and control such processes. Quantifying nutrient and oxygen gradients regulating differentiated and stable biofilms, for example, by using real-time monitoring solutions, would not only aid process development, but will remain key focus.

Financial & competing interests disclosure

The authors have no relevant affiliations or financial involvement with any organization or entity with a financial interest in or financial conflict with the subject matter or materials discussed in the manuscript. This includes employment, consultancies, honoraria, stock ownership or options, expert testimony, grants or patents received or pending or royalties.

No writing assistance was utilized in the production of this manuscript.

Ethical conduct of research

The authors state that they have obtained appropriate institutional review board approval or have followed the principles outlined in the Declaration of Helsinki for all human or animal experimental investigations. In addition, for investigations involving human subjects, informed consent has been obtained from the participants involved.

Executive summary

Background

- An important advantage of membrane-based bioreactors over conventional stirred tank reactors is the provision of an artificial environment for an increased biomass density and enhanced productivity of shear stress-sensitive organisms.
- Innovative bioreactor designs are necessary to derive valuable products, such as secondary metabolites or recombinant proteins from unconventional cell types.

Materials & methods

- A novel capillary ceramic membrane reactor, Quorus gas–liquid–solid, is presented. It provides an ideal platform for the immobilization and cultivation of aerobic and filamentous growing microorganisms as steady-state biofilms.
- The production of recombinant xylanase from *Aspergillus niger* D15 (*xyn2*) was used as a model process to describe the Quorus gas–liquid–solid cultivation conditions.

Results & discussion

- A model to determine the efficiency of this bioreactor in long-term operation is developed. Obtained results are benchmarked to conventional batch processes.
- This bioreactor is ideally suited to the continuous production and harvest of secreted, toxic, labile or volatile products produced by complex microbial biofilms formed by filamentous fungi or actinobacteria.

References

Papers of special note have been highlighted as:
• of interest

1 Kroll S, Meyer L, Graf AM *et al.* Heterogeneous surface modification of hollow fiber membranes for use in microreactor systems. *J. Membr. Sci.* 299, 181–189 (2007).

2 Villain L, Meyer L, Kroll S, Beutel S, Scheper T. Development of a novel membrane aerated hollow-fiber microbioreactor. *Biotechnol. Prog.* 24, 367–371 (2008).

3 Wolff C, Beutel S, Scheper T. Tubular membrane bioreactors for biotechnological processes. *Appl. Microbiol. Biotechnol.* 97, 929–937 (2013).

4 Fan S, Xiao Z, Tang X *et al.* Inhibition effect of secondary metabolites accumulated in a pervaporation membrane bioreactor on ethanol fermentation of *Saccharomyces cerevisiae*. *Bioresour. Technol.* 162(0), 8–13 (2014).

5 Brecht R. Disposable bioreactors: maturation into pharmaceutical glycoprotein manufacturing. In: *Disposable Bioreactors*. Eibl R, Eibl D (Eds). Springer, Berlin, Heidelberg, Germany, 1–31 (2010).

6 Van Geertruyden WH, Huang Z, Clark WR. Hemodialysis membranes: history, properties, and future development. In: *Membrane Technologies and Applications*. Mohanty K, Purkait MK (Eds.). CRC Press, FL, USA, 341–380 (2012).

7 Martin KJ, Nerenberg R. The membrane biofilm reactor (MBfR) for water and wastewater treatment: principles, applications, and recent developments. *Bioresour. Technol.* 122, 83–94 (2012).

8 Ercan D, Demirci A. Current and future trends for biofilm reactors for fermentation processes. *Crit. Rev. Biotechnol.* 1–14 (2013) (Epub ahead of print).

9 Pinzon NM, Cook AG, Ju L-K. Continuous rhamnolipid production using denitrifying *Pseudomonas aeruginosa* cells in hollow-fiber bioreactor. *Biotechnol. Prog.* 29(2), 352–358 (2013).

10 Gross R, Lang K, Bühler K, Schmid A. Characterization of a biofilm membrane reactor and its prospects for fine chemical synthesis. *Biotechnol. Bioeng.* 105(4), 705–717 (2009).

11 Tapia F, Vogel T, Genzel Y *et al.* Production of high-titer human influenza A virus with adherent and suspension

MDCK cells cultured in a single-use hollow fiber bioreactor. *Vaccine* 32(8), 1003–1011 (2014).

12 Wung N, Acott SM, Tosh D, Ellis MJ. Hollow fibre membrane bioreactors for tissue engineering applications. *Biotechnol. Lett.* 36(12), 2357–2366 (2014).

13 Govender S. Biofilm productivity and concomitant cell autolysis in a membrane bioreactor. *Biotechnol. Lett.* 33, 263–271 (2011).

14 Luke AK, Burton SG. A novel application for *Neurospora crassa*: progress from bath culture to a membrane bioreactor for the bioremediatin of phenols. *Enzyme Microb. Technol.* 29, 348–356 (2001).

15 Sheldon MS, Mohammed K, Ntwampe SKO. An investigation of biphasic growth kinetics for *Phanerochaete chrysosporium* (BKMF-1767) immobilised in a membrane gradostat reactor using flow-cells. *Enzyme Microb. Technol.* 42(4), 353–361 (2008).

16 Godongwana B, De Jager D, Sheldon MS, Edwards W. The effect of *Streptomyces coelicolor* development on the hydrodynamics of a vertically orientated capillary membrane gradostat reactor. *J. Membr. Sci.* 333(1–2), 79–87 (2009).

17 Fraser SJ, Endres C. Quorus bioreactor: a new perfusion-based technology for microbial cultivation. In: *Disposable Bioreactors II*. Eibl D, Eibl R (Eds). Springer, Berlin, Heidelberg, Germany, 149–177 (2014).

18 Endres C, Beutel S, Fraser SJ, Edwards W, Scheper T. Produktivitätsanalyse eines neuartigen, nicht begasten keramischen Hohlfaserreaktors. Presented at: *DECHEMA – 27. Jahrestagung der Biotechnologen.* Mannheim, Germany, 8–10 September 2009.

19 Leukes WD, Fraser SJ, Edwards W. WO2007004170 (2007).

20 Ntwampe SKO, Sheldon MS, Volschenk H. The membrane gradostat reactor: secondary metabolite production, bioremediation and commercial potential. *Afr. J. Biotechnol.* 6, 1164–1170 (2007).

- **Provides an additional insight into gradostat process and highlight common misinterpretations of its operational principle.**

21 Govender S, Pillay VL, Odhav B. Nutrient manipulation as a basis for enzyme production in a gradostat bioreactor. *Enzyme Microb. Technol.* 46(7), 603–609 (2010).

- **Gives additional insight into the morphological and physiological impacts on a *Phanerochaete chrysosporium* biofilm during gradostat operation.**

22 De Jager D, Sheldon MS, Edwards W. Modelling growth kinetics of *Streptomyces coelicolor* A3(2) in a pressurised membrane gradostat reactor (MGR). *Enzyme Microb. Technol.* 45, 449–456 (2009).

- **Describes in detail the configuration of single-fiber reactor used in process development of the Quorus gas–liquid–solid processes.**

23 Rose W, Van Zyl S. Constitutive expression of the *Trichoderma reesei* beta-1,4-xylanase gene (*xyn2*) and the beta-1,4-endoglucanase gene (egI) in *Aspergillus niger* in molasses and defined glucose media. *Appl. Microbiol. Biotechnol.* 58, 461–468 (2002).

24 Halan B, Buehler K, Schmid A. Biofilms as living catalysts in continuous chemical syntheses. *Trends Biotechnol.* 30(9), 453–465 (2012).

25 Leukes WD. *Development and Characterisation of a Membrane Gradostat Bioreactor for the Bioremediation of Aromatic Pollutants Using White Rot Fungi [PhD thesis].* Rhodes University, Grahamstown, South Africa (1999).

26 Panikov NS. Kinetics of microbial growth. In: *Upstream Industrial Biotechnology.* Flickinger MC (Ed.). Wiley, NJ, USA, 331–370 (2013).

27 Godongwana B, Solomons D, Sheldon MS. A solution of the convective-diffusion equation for solute mass transfer inside a capillary membrane bioreactor. *Int. J. Chem. Eng.* doi:10.1155/2010/738482 (2010) (Epub ahead of print).

28 Govender S, Jacobs EP, Leukes WD, Pillay VL. A scalable membrane gradostat reactor for enzyme production using *Phanerochaete chrysosporium*. *Biotechnol. Lett.* 25, 127–131 (2003).

29 Su X, Schmitz G, Zhang M *et al.* Heterologous gene expression in filamentous fungi. *Adv. Appl. Microbiol.* 81(1), 1–61 (2012).

30 Fleißner A, Dersch P. Expression and export: recombinant protein production systems for *Aspergillus*. *Appl. Microbiol. Biotechnol.* 87(4), 1255–1270 (2010).